Scientific Research and Essays Vol. 5(10), pp. 1084-1099, 18 May, 2010
Available online at http://www.academicjournals.org/SRE
ISSN 1992-2248 © 2010 Academic Journals

Full Length Research paper

DSP implementation of underwater communication using SSB modulation with random carrier frequencies

Murat Kuzlu[1]*, Hasan Dinçer[2] and Sitki Öztürk[2]

[1]Department of Power Electronics and Control, TUBITAK-MRC Energy Institute, Kocaeli, Turkey.
[2]Department of Electronics and Telecommunications Engineering, Kocaeli University, Kocaeli, Turkey.

Accepted 26 April, 2010

Underwater acoustic communication is a rapidly growing field of research and applied engineering. It is especially necessary for submarine-ship, submarine-submarine and ship-submarine communications. Recent years have seen rapid advances in DSP (Digital signal processor) architecture technologies, which advances have made it possible for DSP's to be used for applications previously considered unsuitable such as underwater communication. Underwater acoustic communication applications had been performed in an analog environment several times before; however, in this work, it is performed digitally by using DSP. Alternative solutions for underwater communication are presented as well. The presented solution is a more reliable prototype design of underwater acoustic communication that was developed via the transmitter and receiver sides on two identical DSK (DSP Starter Kit) boards by using upper sideband - suppressed carrier (SSB - SC) and random carrier frequencies (8 kHz - 16 kHz).

Key words: Underwater acoustic communication, underwater telephone (uwt), digital signal processor.

INTRODUCTION

The need for underwater wireless communications exists in applications such as remote controls in off-shore oil industry, pollution monitoring in environmental systems, collection of scientific data recorded at ocean-bottom stations and by unmanned underwater vehicles, speech transmission between divers, and mapping of the ocean floor for objects detection and recovery. Wireless underwater communications can be established by transmission of acoustic waves. Radio waves are of little use because they are severely attenuated, while optical waves suffer from scattering and need high precision in pointing the laser beams. Underwater acoustic communication channels are far from ideal.

They have limited bandwidth and often cause severe signal dispersion in time and frequency (Brekhovskikh and Lysanov, 1982; Quazi and Konrad, 1982; Catipovic, 1990; Baggeroer, 1984; Stajanovic, 1996). For instance, energy absorption at f = 10 kHz is 3000 dB/km for electromagnetic waves and only 1 dB/km for sonic waves. Thus, using an acoustic carrier is considerably more energy-efficient than the use of electromagnetic radiation (Zielinski, 2004). Among the first modern underwater communication systems was an underwater telephone, which was developed in the forties in the United States for communication with submarines. This device used a single side band (SSB) suppressed carrier amplitude modulation in frequency range 8 - 11 kHz and it was capable of sending an acoustic signal over several kilometers (Istepanian and Stojanovic, 2002).

Most of the current underwater acoustic solutions utilize analog techniques. Some common drawbacks with traditional analog implementations include accuracy limitations due to circuit complexity, device tolerances, and sensitivity to electrical noise. Digital signal processing addresses most of these limitations (Yagnamurthy, 2003).

Sound is disturbances of the medium. Here water travelling in a 3 dimensional manner as the disturbance propagate with the speed of sound. Acoustic impedance is one of the most basic concepts of underwater sound because its definition is a constitutive equation (one from which others are derived) for underwater sound propagation. The relation is:

$$Z_a = \rho.c \quad (1)$$

*Corresponding author. E-mail: mkuzlu@hotmail.com.

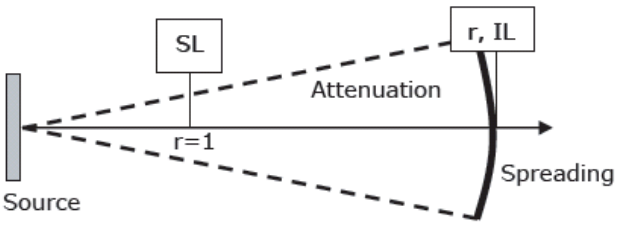

Figure 1. Schematic of sound transmission with spreading (Reson Inc., 2009).

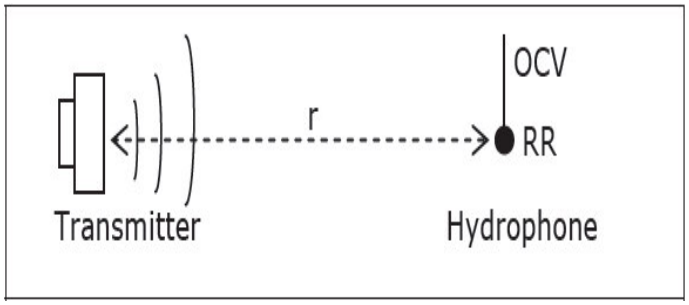

Figure 2. Transducer transmitting of the underwater sound (Reson Inc., 2009).

This definition is analogous to Ohm's law for electrical circuits that is, V = R.I and particle velocity (c), acoustic impedance (Z_a) and sound pressure (ρ) can be thought in the same way. It shows that particle velocity and pressure are in phase in a plane sound wave.

Acoustic intensity - power (P_a) per unit area (A_a) or energy flux - is used to describe levels of underwater sound that is, an echo, a whale's call or a signal from a remote transducer. The intensity of a plane harmonic wave is:

$$I_a = \frac{P_{rms}^2}{\rho.c} = \frac{P_a}{A_a} \quad (2)$$

The daily term "a high sound" refers to a sound with a high intensity. A reference intensity I_{ref} has been defined in order to enable direct comparison of the loudness of sounds and the reference intensity used in underwater acoustics is that of a plane harmonic wave with an rms-pressure of 1 *µPa*, which for ordinary seawater with *c* ≈ 1500 m/s and ρ ≈ 1000 kg/m^3 gives (Reson Inc., 2009).

$$I_{ref} = \frac{(1\mu P_a)^2}{1000.1500} = 0{,}667.10^{-18}(w/m^2) \quad (3)$$

The intensity level (IL) is the intensity of the sound wave taken in decibels relative to the reference intensity of 1 *µPa* plane wave rms-pressure (which is shortened to "re 1 *µPa*"):

$$IL = 10\log\frac{1}{0.667.10^{-18}}\, dB\ re\ 1\mu P_a \quad (4)$$

Sounds originating from acoustic sources are measured in intensity level, which decreases as the distance to the source is increased due to transmission loss (TL) that is, spreading and absorption:

$$IL = SL - TL = SL - 20\log(r) - \alpha(r - 1m) \quad (5)$$

The formula assumes spherical spreading for the transmission loss that is, the sound is unbounded and spreads out as it was originating from a point, the acoustic center of the source. Schematic of sound transmission with spreading is shown in Figure 1.

Spherical spreading is most common and is valid in the far field provided that the source is placed far enough from any large structure. The last term of the transmission loss is the attenuation, which increases very significantly with the frequency and furthermore varies with pressure, temperature, salinity and acidity.

The transmitted voltage response, TVR, is defined in such a way that the source level can be calculated from:

$$SL = TVR + 20\log(V_{rms}) \quad (6)$$

The TVR value is often measured at low power and since the electric-to-acoustic efficiency can drop significantly with increased power levels it is often best to use the TVR relation with caution. Transducer transmitting of the underwater sound is shown in Figure 2. The source level (SL) of a transmitter can be estimated (ignoring attenuation) by measuring the output voltage (OCV) of a hydrophone submerged in the vicinity of the transmitting transducer and the receiver response (RR) of transducer:

$$SL = 20\log(OCV) - RR + 20\log(r/1m) \quad (7)$$

DESIGN AND THE LOWER PARTS OF THE DSP

IMPLEMENTATION

In this section, we describe design and the lower parts of the implementation. While creating embedded system pieces, acoustic underwater communication software was created by choosing an effective and capable DSP. This embedded system software was written in the (Texas, TMS320VC5509A) DSP environment which is called Spectrum Digital, 5509A DSK. The 5509A DSK is a low-cost standalone development platform that enables users to evaluate and develop applications for the TI C55XX DSP family (Spectrum Digital Inc., 2005). One of the key components of the implementation is the audio signal input/output module. The 5509A development board we used has a built-in module for sampling

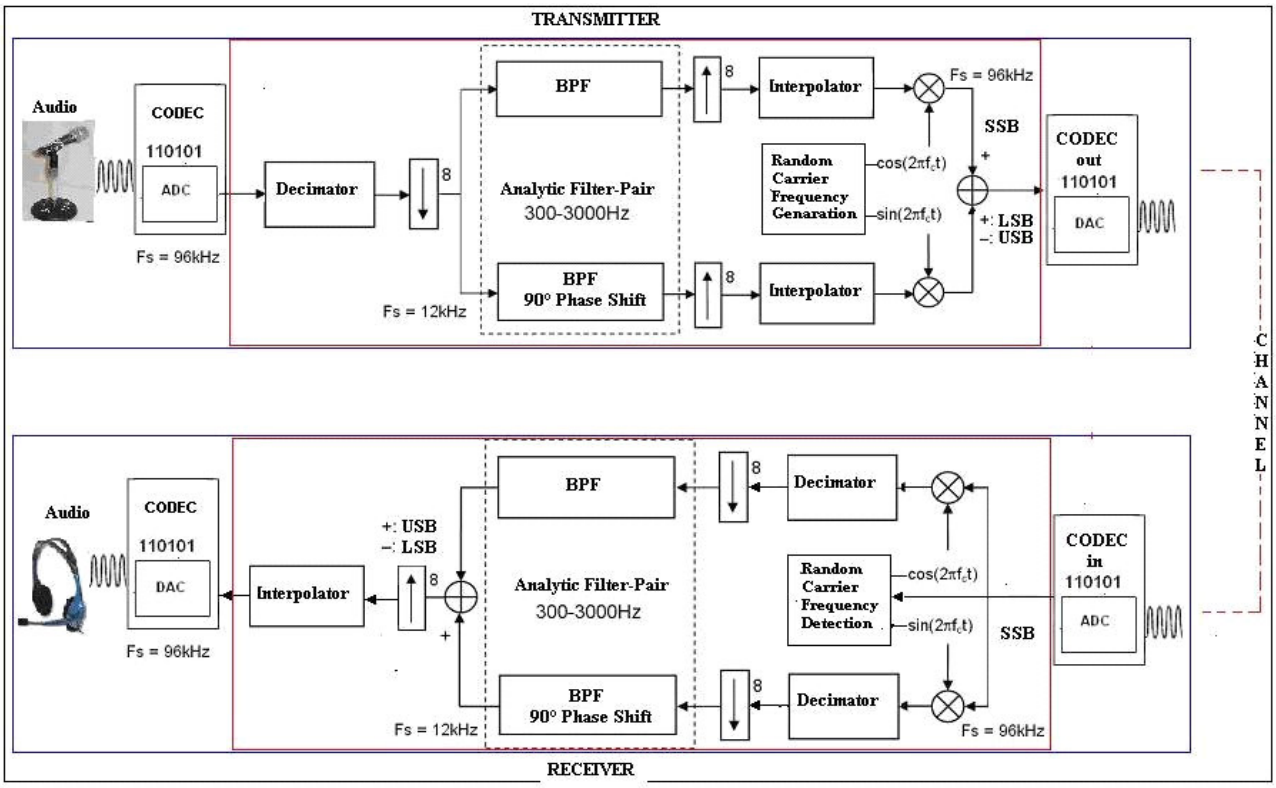

Figure 3. Block diagram of DSP implementation.

and generating audio signals. The tasks are handled by the integrated TLV320AIC23 codec, a high-performance stereo audio codec with highly integrated analog functionality. Data-

transfer word lengths of 16, 20, 24, and 32 bits, with sampling rates from 8 to 96 kHz, are supported (Texas Instruments Inc., (2002).

Using CODEC integrated circuits which are typically used for sound applications, converting sound signals to digital signals and converting modulating/demodulating signals to sound signals are operated with high quality and simply.

Texas DSPLIB library version 2.31 was used for FFT and FIR filtering. Filters were obtained in MATLAB and coefficients were transferred to the software. Digital signal processing library (DSPLIB) provides a set of C-callable, assembly-optimized functions commonly used in signal processing applications, e.g. filtering and transform. The DSPLIB includes several functions for each processing category, based on the input parameter conditions, to provide parameter-specific optimal performance (Texas Instruments Inc., 2006).

Design of DSP implementation using random carrier frequencies in a test pool

Block diagram of DSP implementation using random carrier frequencies in a test pool is shown in Figure 3. In implementation there are two sides as transmitter and receiver and each processing step meet each other on transmitter and on receiver. The microphone is selected as the audio signal source. The sampling rate is set to 96 kHz and the data word length is set to 16 bits. To sample audio signals, one of the multichannel-buffered serial ports (McBSP) is configured to connect the AIC23 codec. The audio data is transferred between the codec and the internal L2 memory through the direct memory access (DMA) channels continuously save the raw audio data from the AIC23 codec. When one of the two buffers is filled, a DMA interrupt is initiated and the data is passed to the interrupt service routine (ISR) and then is processed. At the same time, the codec keeps the sampling and the saves data in the other buffer. So data sampling and processing can be performed simultaneously and no incoming signals are missed even if the DSP is processing previously received data.

Analog audio signal coming from microphone input of the AIC23 codec is converted to digital signal by analog-to-digital converter (ADC) of the AIC23 codec. Then this digital signal is sent to the DSP via McBSP serial port interface to perform decimation/ interpolation filtering, mixer and modulation/demodulation processing. Sampling frequency of the digital signal is decreased to 12 kHz by a decimation filter. This is exactly same as running the decimation filter at the lower rate. This method is typical of those used by DSP designers to save time and effort.

There are two signal processing channels as I (In Phase) and Q (Quadrature) channels. Band pass filter (300 - 3000 Hz) is applied to both I and Q channels. Additional hilbert transformation is applied to the Q channel, too. After band pass filtering operation, the sampling frequency of digital signal must be increased to mix with high frequency carrier signal. An interpolation filter is naturally required. It is particularly convenient to choose an interpolation factor of 8 to increase the sampling rate to 96 kHz. Bandwidth is expanded to 48 kHz by increasing the sampling frequency of signal so that signals with higher carrier frequency can be sent and received. Then a high-frequency signal is mixed with carrier signal obtained using “Random Carrier Frequency Generation” algorithm. This implementation is for upper side-band modulation. According to USB modulation, I and Q signals are subtracted from each other for transmitter side. Thus, only the upper side band signal remains and the bandwidth can be used more efficiently. At this point USB

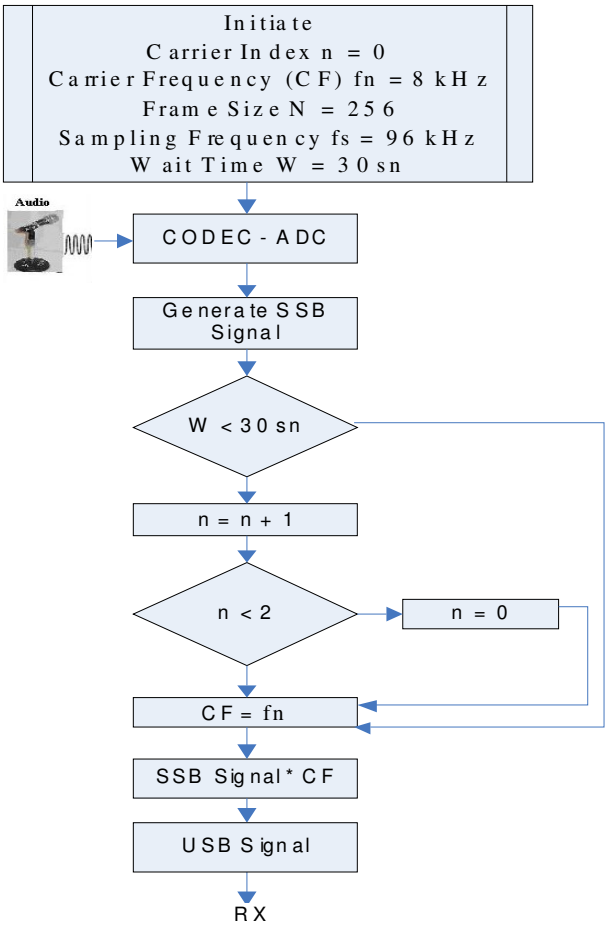

Figure 4. "Random carrier frequency generation algorithm" for transmitter.

signal is generated and all operations are completed on transmitter side. The modulated signal must be sent to the receiver side. It is performed by sending the modulated signal from line out of DSK1 (transmitter) AIC23 codec to input of power amplifier. USB signal is amplified approximately 50 times by power amplifier. Then amplified signal is amplified three times by a transformer again for impedance matching. Lastly amplified analog signal is sent by B&K 8103 transducer in a test pool via underwater.

Modulated signal is received on the receiver side. Same B&K 8103 transducer is used on receiver side. Received signal by B&K 8103 transducer is amplified approximately 200 times by pre-amplifier. Then amplified signal is sent to line in of DSK2 (receiver) AIC23 codec. Firstly ADC of the AIC23 codec for each frame size converts the received signal to digital signal. After converting process, digital signal is mixed by the carrier signal obtained using "Random Carrier Frequency Detection" algorithm for I and Q channels. Then high-frequency signal is converted to low-frequency signal. So sampling frequency of the digital signal is decreased by the decimation filter to 12 kHz and low frequency signal is obtained. Band pass filter (300 - 3000Hz) is applied to these signals on both I and Q channels. Additional hilbert transformation is applied to the Q channel as on transmitter side. After all operations are completed for two channels, according to USB demodulation, I and Q signals are added together to regenerate the original signal for receiver side. Sampling frequency of regenerated original signal is increased to 96 kHz. Then the digital signal is sent to AIC23 codec via the McBSP interface. Finally, the original signal is obtained but it is still digital signal. So it must be converted to analog signal. Digital signal is converted to analog signal by digital-to-analog converter (DAC) of AIC23 codec and user can listen to analog audio via headphone of the AIC23 codec.

Analytic filter-pair

Each filter has the same frequency response as the other; they differ only in their phase responses. We begin by designing a low-pass filter having the desired transition-band characteristic, H(w); we obtain its impulse response, h(t). Multiplying the impulse response by a complex sinusoid of angular frequency, w_0 results in two sets of coefficients one for the real part and one for the imaginary part.

The I filter has a phase response differing 90° at every frequency from the Q filter. The frequency translation theorem works just as well on the responses of filters as it does on real signals. To perform this transformation of the L coefficients of the prototype LPF, new coefficients are calculated according to:

$$0 \le k \le L-1$$

$$hI(k) = h(k) \cdot \cos\left[\omega_o\left(k - \frac{L}{2} + \frac{1}{2}\right)t_s\right] \quad (8)$$

$$hQ(k) = h(k) \cdot \sin\left[\omega_0\left(k - \frac{L}{2} + \frac{1}{2}\right)t_s\right] \quad (9)$$

where t_s is the sampling period. When the low-frequency transition band is placed near zero frequency, as we would like for SSB, the BW of each BPF is approximately twice that of the prototype LPF (http://yb1zdx.arc.itb.ac.id/data/ OWP/arrl-books/arrl-handbook-2005/16.pdf, 2009). SSB is key point of performing modulation and demodulation process for underwater acoustic communications. SSB modulation/demodulation process can be easily performed using the analytic filter-pair.

Random carrier frequency generation algorithm

"Random Carrier Frequency Generation Algorithm" is shown in Figure 4. Carrier frequency generation algorithm is processed on transmitter side. In this algorithm, two carrier frequencies (8 - 16 kHz) are defined. The code which runs on DSP controls signal's frame number if 30 s passed. After each 30 s, carrier frequency index is increased and the signal is provided to be sent by next carrier frequency. When carrier index reaches 2, then again index become 0. Loop continues and repeats itself.

Random carrier frequency detection algorithm

"Random Carrier Frequency Detection Algorithm" is shown in Figure 5. Random carrier frequency detection algorithm is processed on receiver side. Fast Fourier Transform (FFT) operation is applied to receive 256 frames by this algorithm. To control silence situation, maximum FFT value is controlled. If maximum FFT value is under threshold level, carrier frequency is accepted as previous carrier frequency and demodulation operation is processed by previous carrier frequency. If maximum FFT value is above threshold level, the maximum valued index is found. This index is multiplied by unit frequency interval and found estimated carrier frequency. If estimated carrier frequency is one of the known carrier frequencies. It is set as the new carrier frequency and demodulation procedure

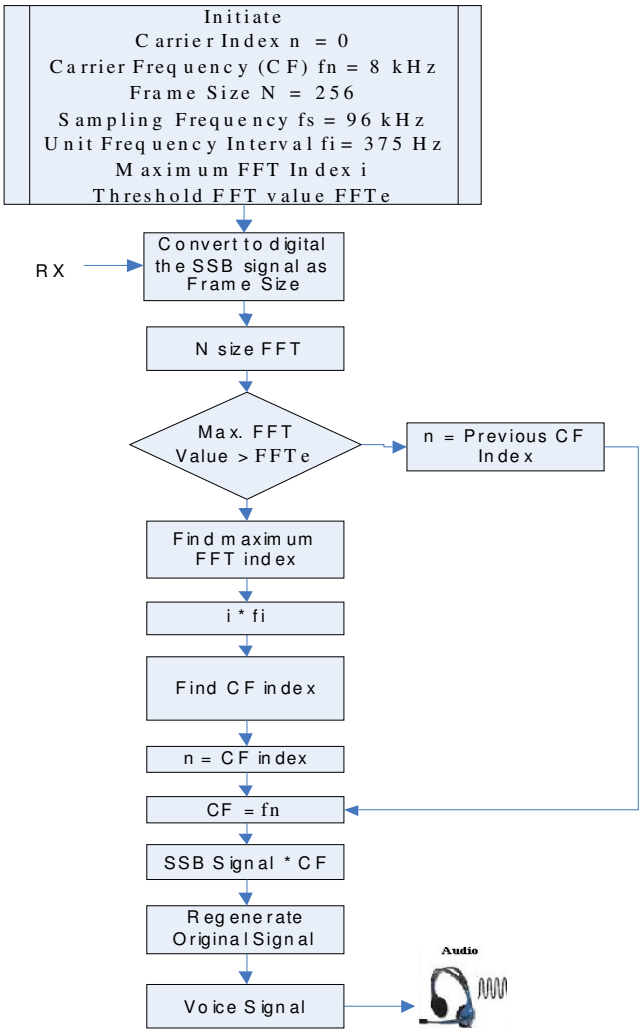

Figure 5. "Random carrier frequency detection algorithm" for receiver

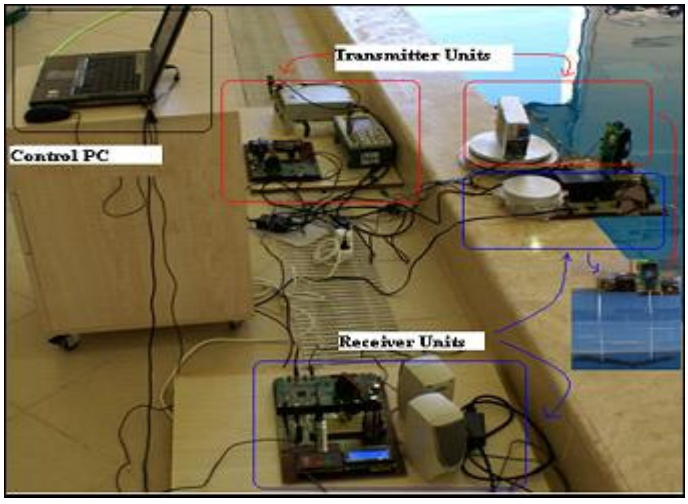

Figure 6. The DSP based prototype for underwater acoustic communication.

is continued with this frequency. FFT is key point of detecting the carrier frequencies by "Random Carrier Frequency Detection Algorithm". A Fourier transform is a mathematical technique for determining the frequency content of a signal.

DSP implementation prototype

Figure 6 shows the DSP implementation prototype for underwater acoustic communication. DSP implementation consists of two 5509A DSK boards, two amplifiers, two transducers, two LCD Displays, two Keypads, two headsets and two cables.

The design of modern data transmission systems has been accompanied by extensive research to achieve high data rates by channel equalization, array processing, phase steering and adaptive beam forming. Although these methods may be beneficial in communication applications for autonomous underwater vehicles, neither array processing nor adaptive beam forming is suitable due to the increased signal processing complexity and physical size of the system (Istepanian and Stojanovic, 2002). Therefore omni-directional transducers are used on both receiver and transmitter side in this implementation.

RESULTS AND DISCUSSION

In this section, we gave the results in a test pool for different frequencies and the results of two DSK's using a 16 kHz random carrier frequency in a test pool. Then we compared mathematically calculated values by formulas and calculated values by measurements.

The results in a test pool for different frequencies

The results for different frequencies were compared to mathematically calculated values. Before these measurements, some values should be handled. Receiver sensitivity of used frequencies according to transducer's transmitter, receiver response and power while broadcasting in 1 V reference value should be known. Besides, the gain parameters of amplifiers on the transmitter and the receiver side should be known. Lastly, distance of measurement and transducer's input voltage were used in measurements. In Tables 1, 2 and 3, list of hydrophone received response, list of power amplifier circuit gain to frequencies and list of pre-amplifier circuit gain to frequencies are shown respectively.

Values which are shown in tables were already known values and were used in measurements. These values are directly related with voltage which is applied to transducer in transmitter amplifier output. Basic parameters of implementation are transmit voltage response TVR, transducer input voltage $V_{rms,}$ hydrophone received response RR, pre amplifier gain G_{pamp}, open circuit (output) voltage OCV, power efficiency $P_{e.}$

For transmitter side hydrophone intensity level (IL) at r meter distance and source level (SL):

$$SL = TVR + 20\log(V_{rms}) + P_e \quad (10)$$

$$IL = SL - TL = SL - 20\log(r) \quad (11)$$

Table 1. List of the hydrophone received response (Brüel and Kjær Inc., 2009).

Frequency (kHz)	Sensitivity dB re 1 V/ µPa - RR	Frequency (kHz)	Sensitivity dB re 1 V/ µPa - RR
8	-210.4	16	-211.3

Table 2. List of power amplifier gain to frequency (Brüel and Kjær Inc., 1992).

Frequency (kHz)	Transmit voltage response - dB re µPa /V @ 1m - TVR	Frequency (kHz)	Transmit voltage response - dB re µPa /V @ 1m – TVR
8	89	16	101

Table 3. List of pre amplifier gain to frequency.

Frequency (kHz)	Gain - G_{pamp} (dB)	Frequency (kHz)	Gain - G_{pamp} (dB)
8	189 (45.52)	16	130 (42.27)

Here, SL was known and IL was predicted for transmitter side. Similarly, for receiver side hydrophone intensity level (IL) and source level (SL):

$$IL = 20\log(OCV) - RR \quad (12)$$

$$SL = 20\log(OCV) - RR + 20\log(r) \quad (13)$$

Here, IL was known and SL was predicted for receiver side. These values were calculated when gain levels were not considered. Results of measurement in time and frequency domain for 8 and 16 kHz are shown in Figures 7 and 8, respectively.

Transmitter and receiver side's signal levels were calculated according to measurement results. RIL shows hydrophone intensity level of r meter distance for transmitter side and TSL shows source level for receiver side.

$$RIL = TVR + 20\log(V_{rms}) - 20\log(r) \quad (14)$$

$$TSL = 20\log(OCV) - RR - Gpamp + 20\log(r) \quad (15)$$

Some values were constant for all frequencies and were not changed. Here, these values are Gpamp and r. Value of r is fixed 25 cm in measurements. Values which were changed according to frequencies TVR, RR and Gpamp were processed according to each measurement reference value. According to constant values and to given formulas, P_e value changes according to hydrophone input impedance and power amplifier output impedance. Decibel (dB) level of power amplifier was set 34 dB due to high input impedance of hydrophone.

$$RIL = TVR + 20\log(V_{rms}) - 34 + 12$$

$$TSL = 20\log(OCV) - RR - Gpamp - 12$$

For 8 kHz signal, TVR = 89 dB re µPa /V @ 1m, V_{rms}=60.6 V, RR = -210.4 dB re 1 V/ µPa, OCV = 4.3 mV_{rms} (6.1 mV_{max}), G_{pamp}= 45.52 dB accordingly

$$RIL = 89 + 35.6 - 22 = 102.6 \ \ dB$$

$$TSL = -47.3 + 210.4 - 45.52 - 12 = 105.58 \ \ dB$$

For 16 kHz signal, TVR = 101 dB re µPa /V @ 1m, V_{rms}=59.4 V, RR = -211.3 dB re 1 V/ µPa, OCV = 8.24 mV_{rms} (11.77 mV_{max}), G_{pamp} = 42.27 dB accordingly

$$RIL = 101 + 35.47 - 22 = 114.47 \, dB$$

$$TSL = -41.68 + 211.3 - 42.27 - 12 = 115.35 \, dB$$

All measurements were realized in a test pool. Desired frequencies were generated using signal generator and applied to power amplifier input. Then, output of amplifier was applied to hydrophone input and was sent via underwater acoustics. At receiver side, this signal was received by hydrophone and was read by DSP. Measurement results that RIL and TSL values are close each other and small differences are derived from producers' tolerance of hydrophone density level, amplifier gains and power efficiency.

The results of two DSK using a 16 kHz random carrier frequency in a test pool

This application was simulated via Matlab before performing on DSK boards. SSB modulation and demodulation results were examined. The application was performed by DSK boards with transmitter and receiver transducers.

Basic parameters of implementation: Sampling Frequency Fs: 96 kHz, Bit Resolution nbit: 16, Buffer Size BUFFSIZE: 512, FFT Length N: 256, Carrier Frequency Index n: 2, Carrier Frequencies fcf: 8 kHz – 16 kHz, Unit Frequency Interval df: 375 Hz. DSP implementation results are as shown in the following figures. Frequency response of signal was obtained using random carrier frequency detection algorithm as shown in Figure 9. Maximum FFT value of received signal is around 16 kHz.

All steps of SSB demodulation are shown in the following figures. In Figures 10, 11, 12, 13, 14 and 15

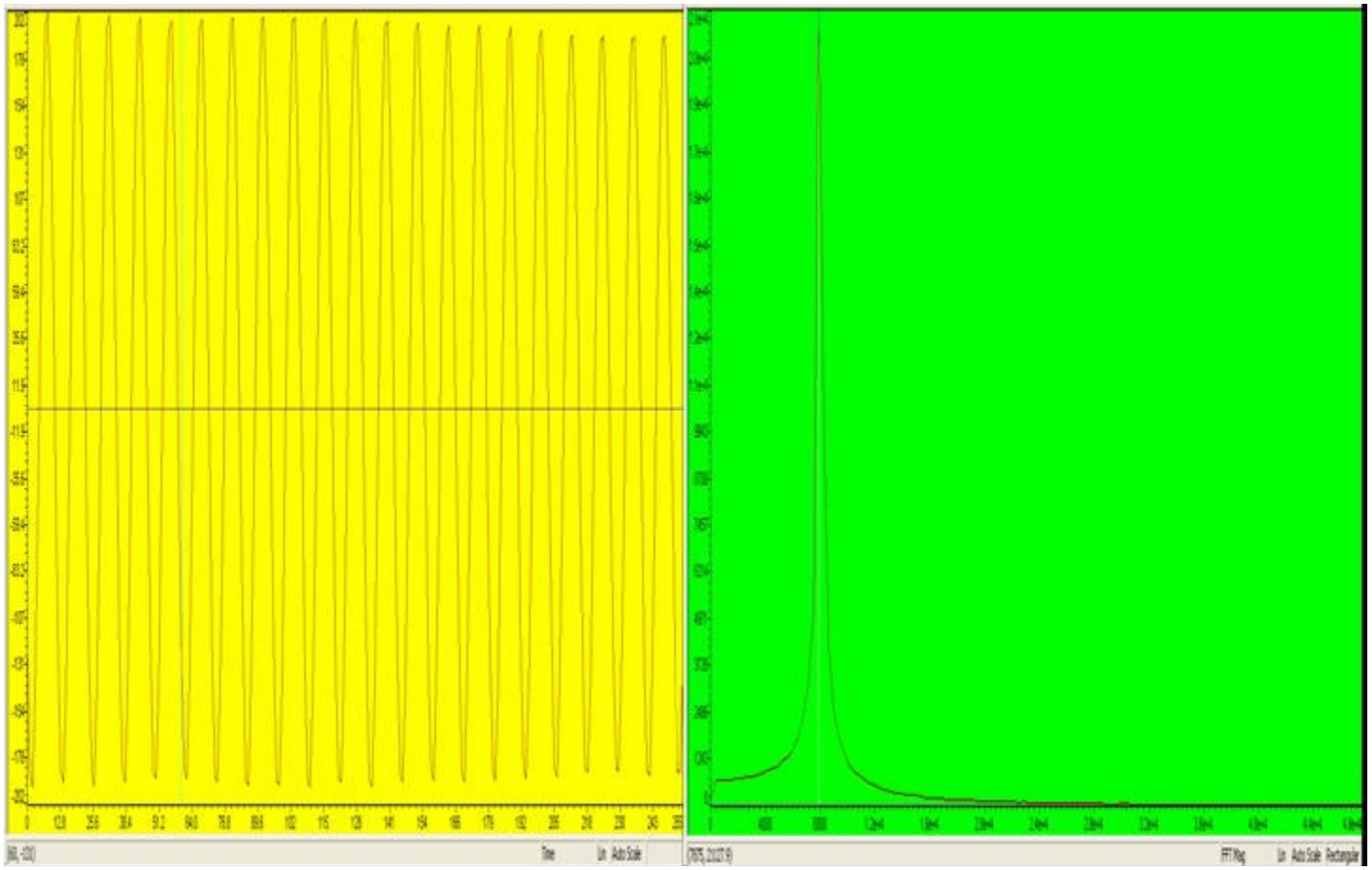

Figure 7. Time and frequency response of result of test pool at 8 kHz.

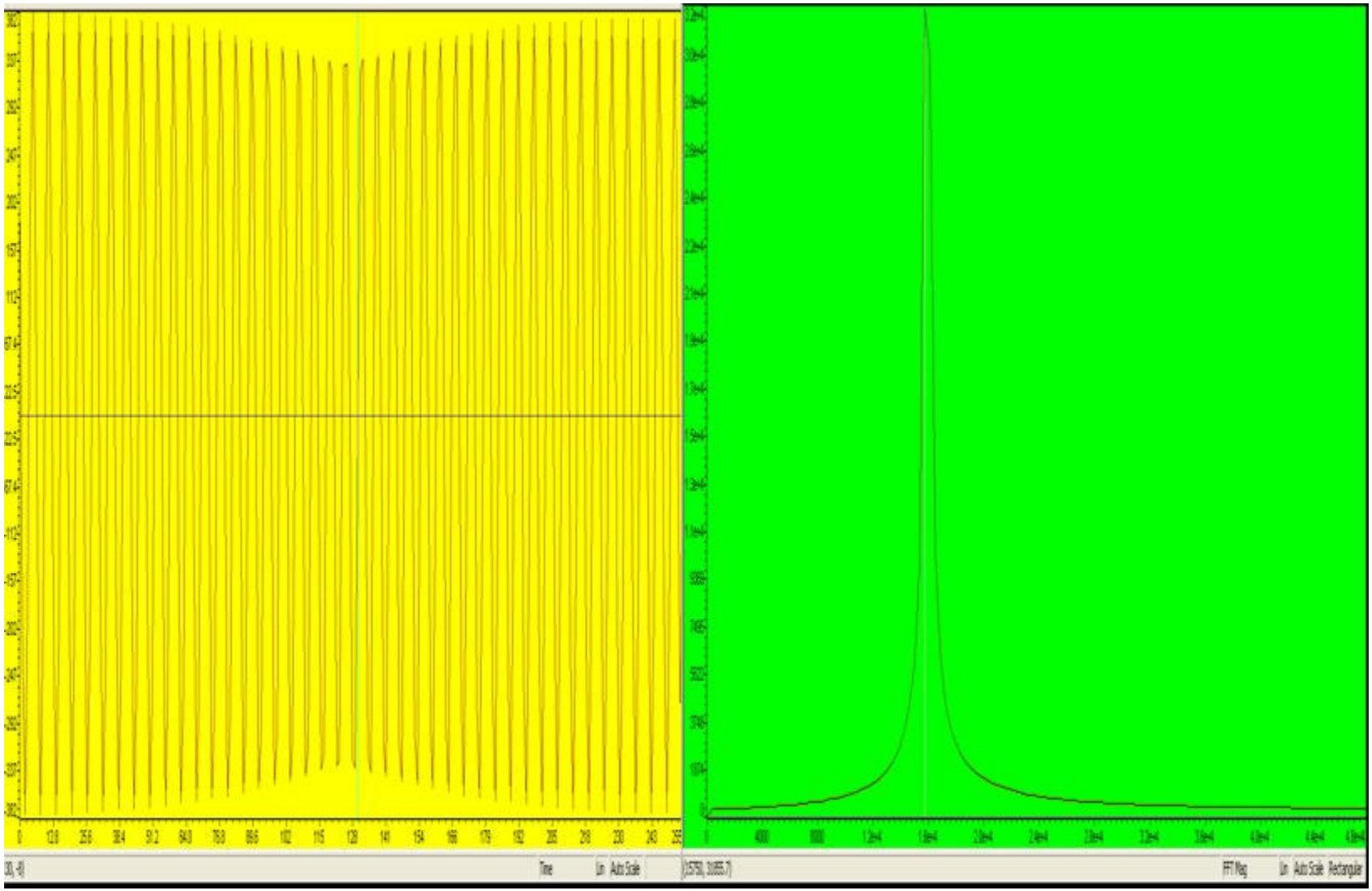

Figure 8. Time and frequency response of result of test pool at 16 kHz.

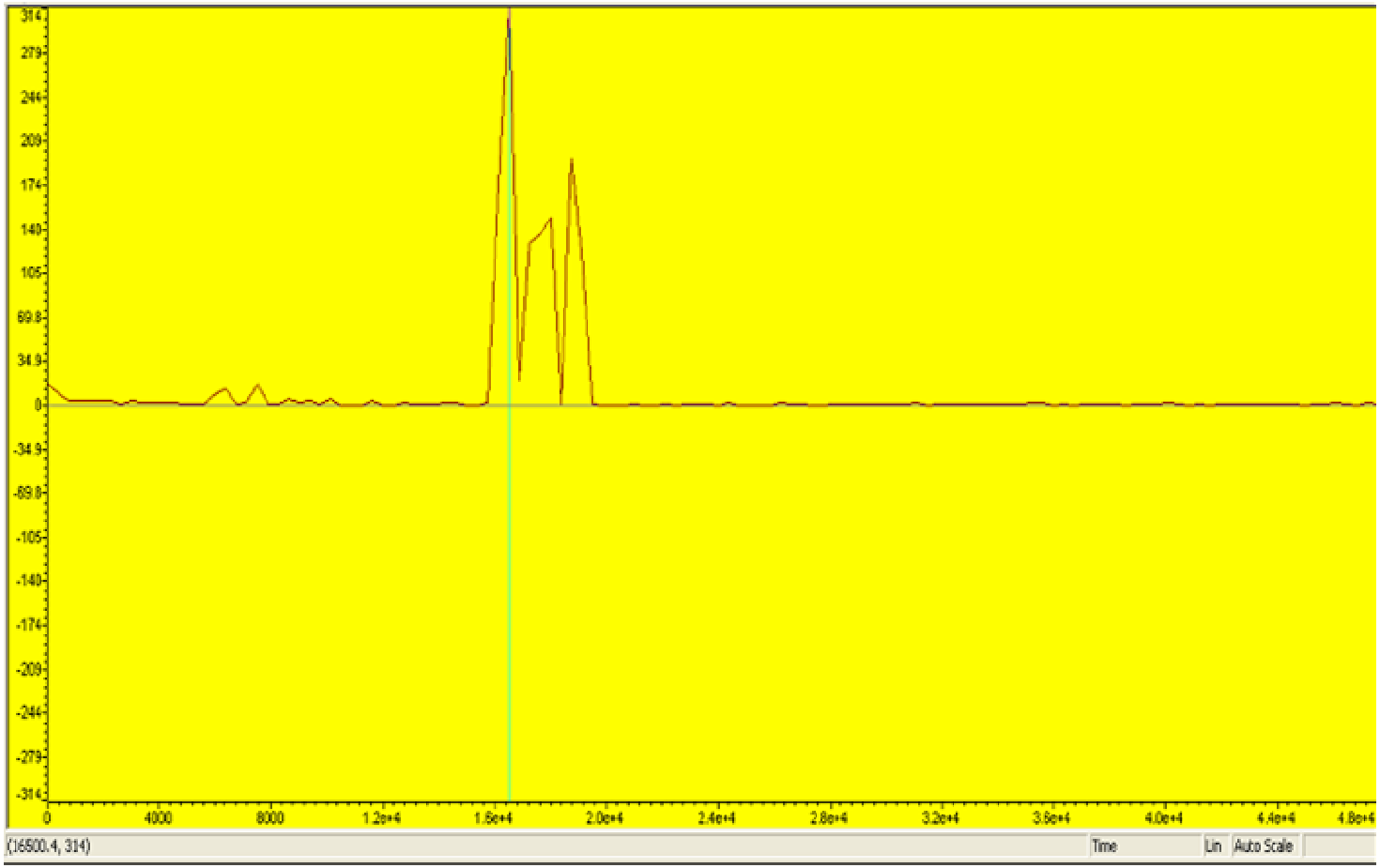

Figure 9. Frequency response of signal that obtained using random carrier frequency detection algorithm.

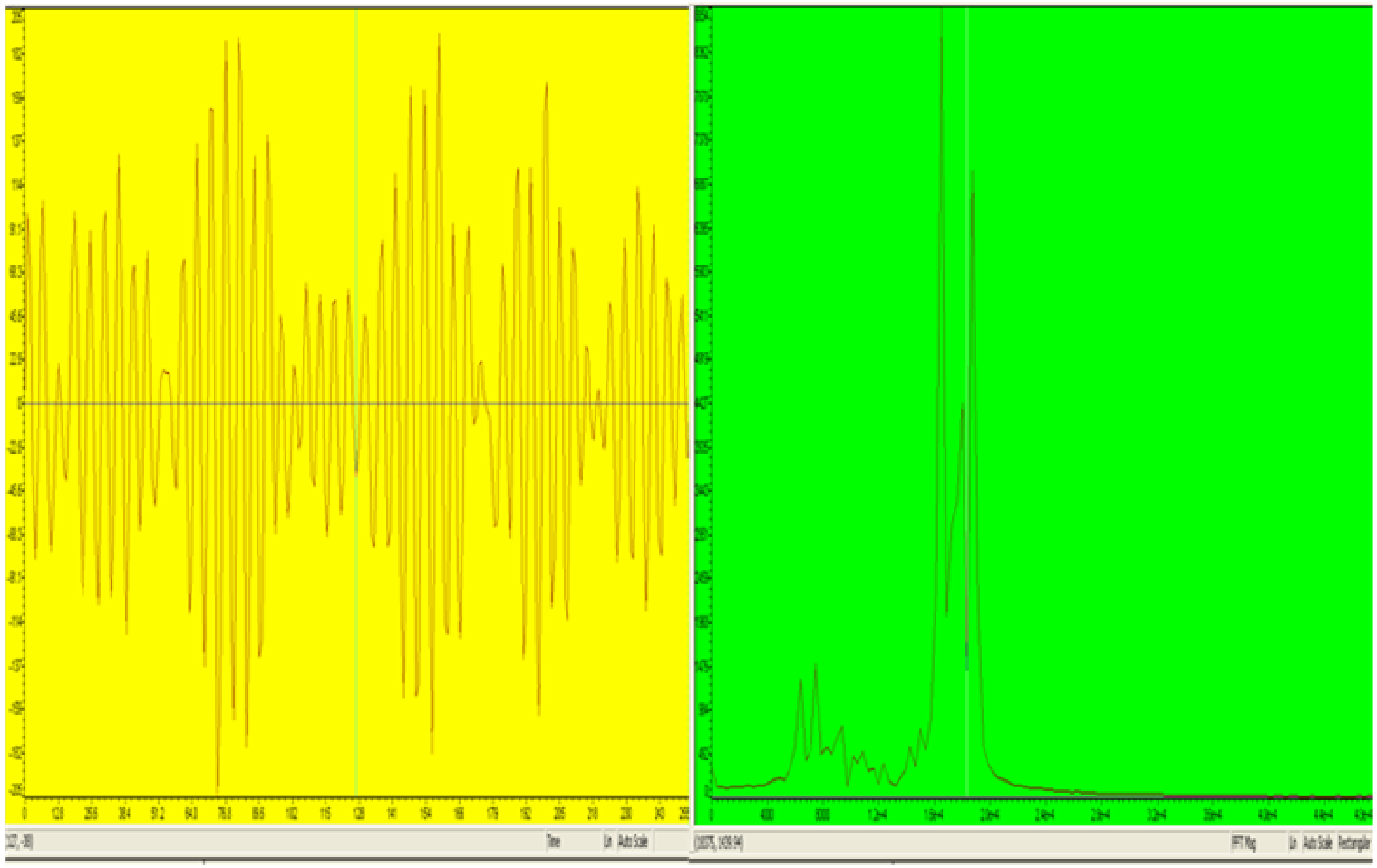

Figure 10. Time and frequency response of modulated USB signal.

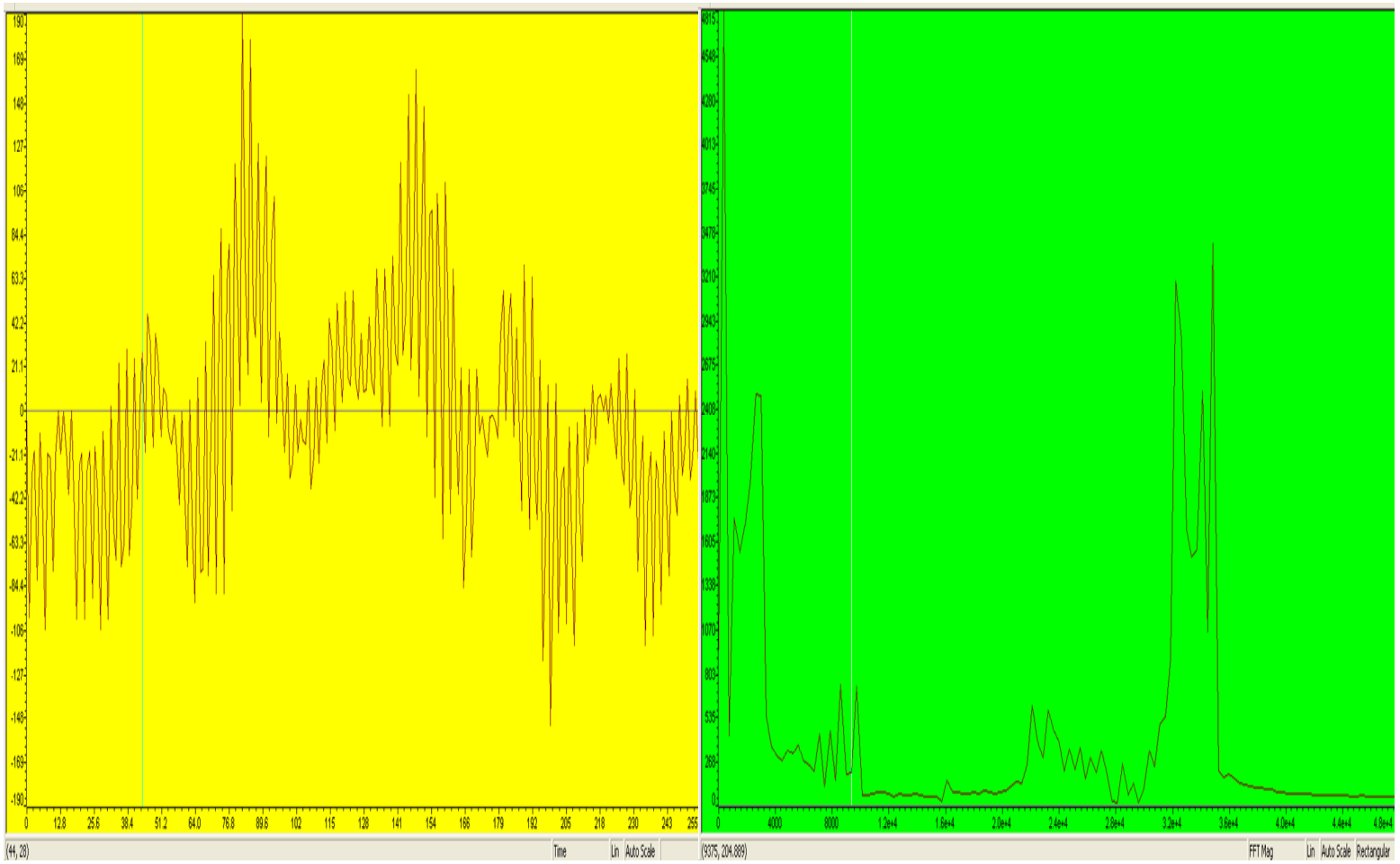

Figure 11. Time and frequency response of mixed received signal with carrier signal in I channel.

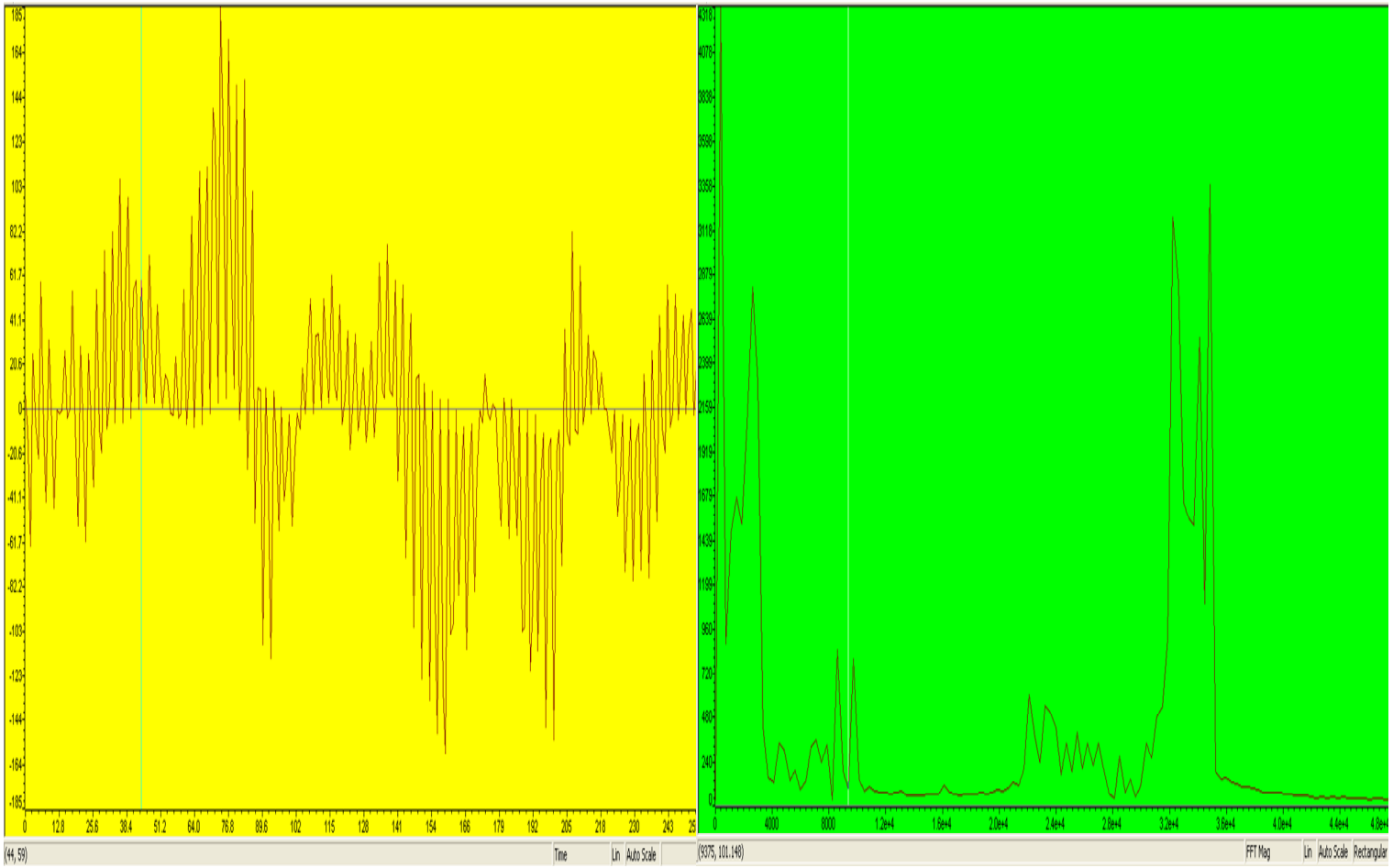

Figure 12. Time and frequency response of mixed received signal with carrier signal in Q channel.

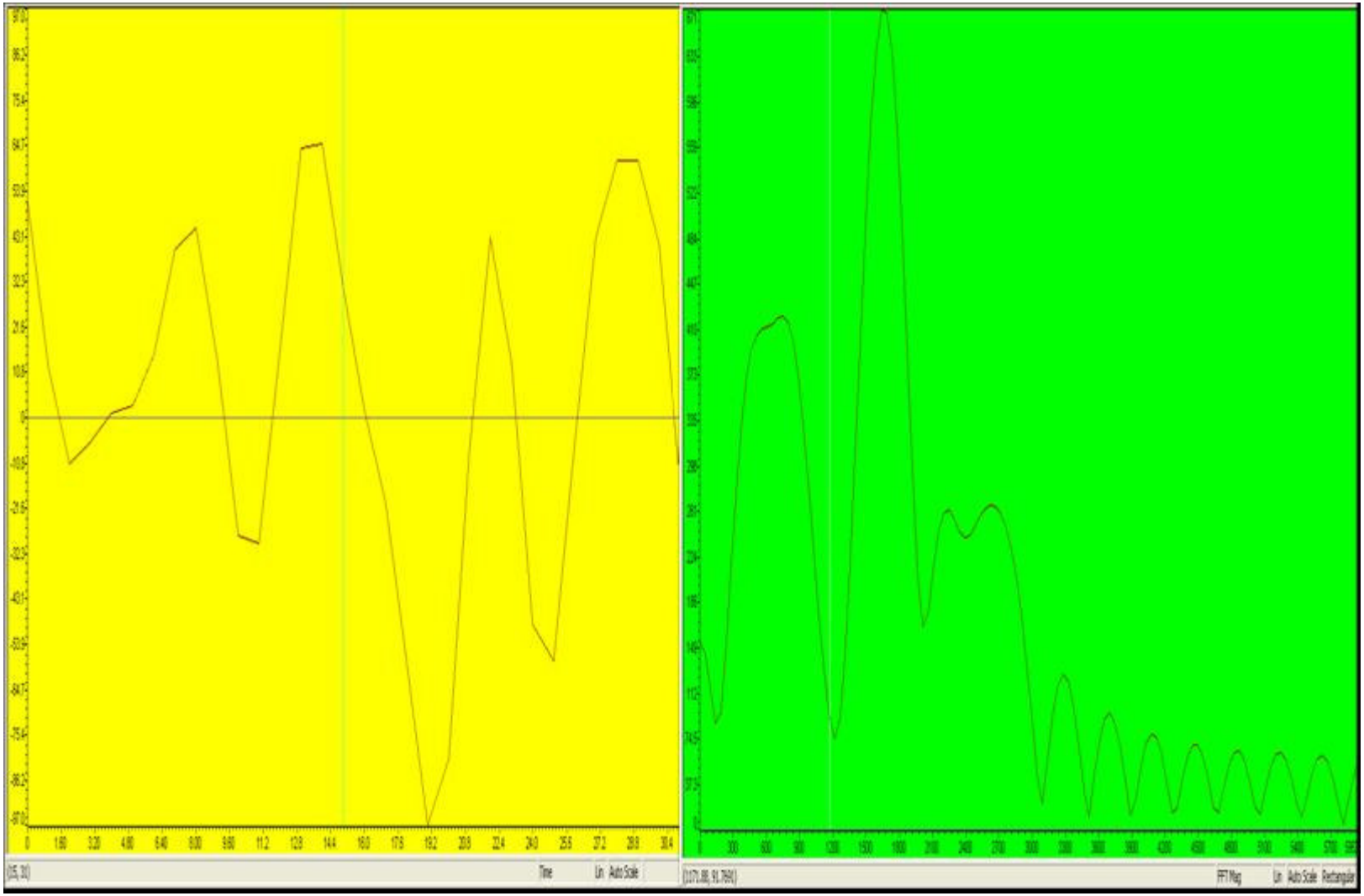

Figure 13. Time and frequency response of BPF signal in I channel.

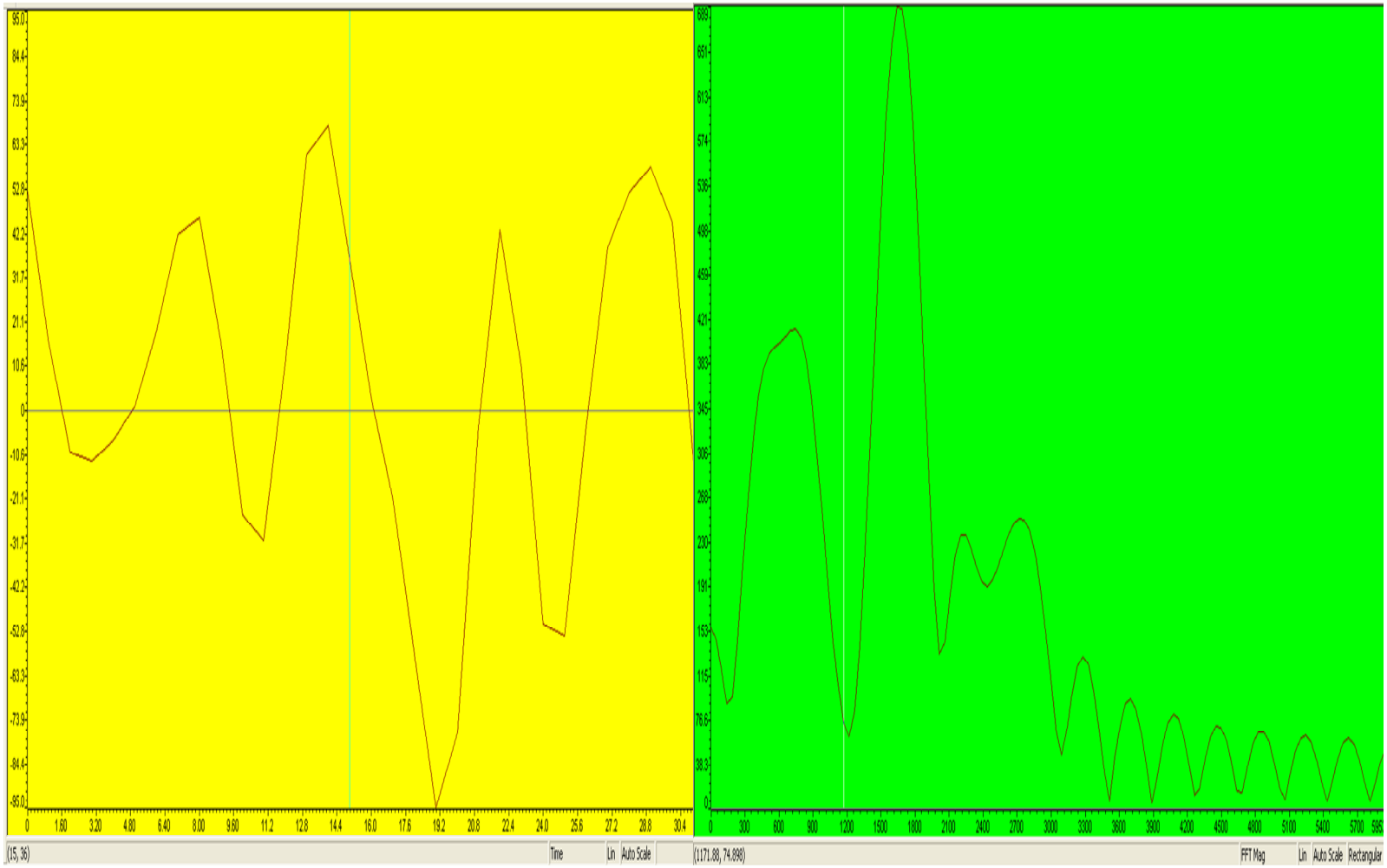

Figure 14. Time and frequency response of BPF and Hilbert Transform signal in Q channel.

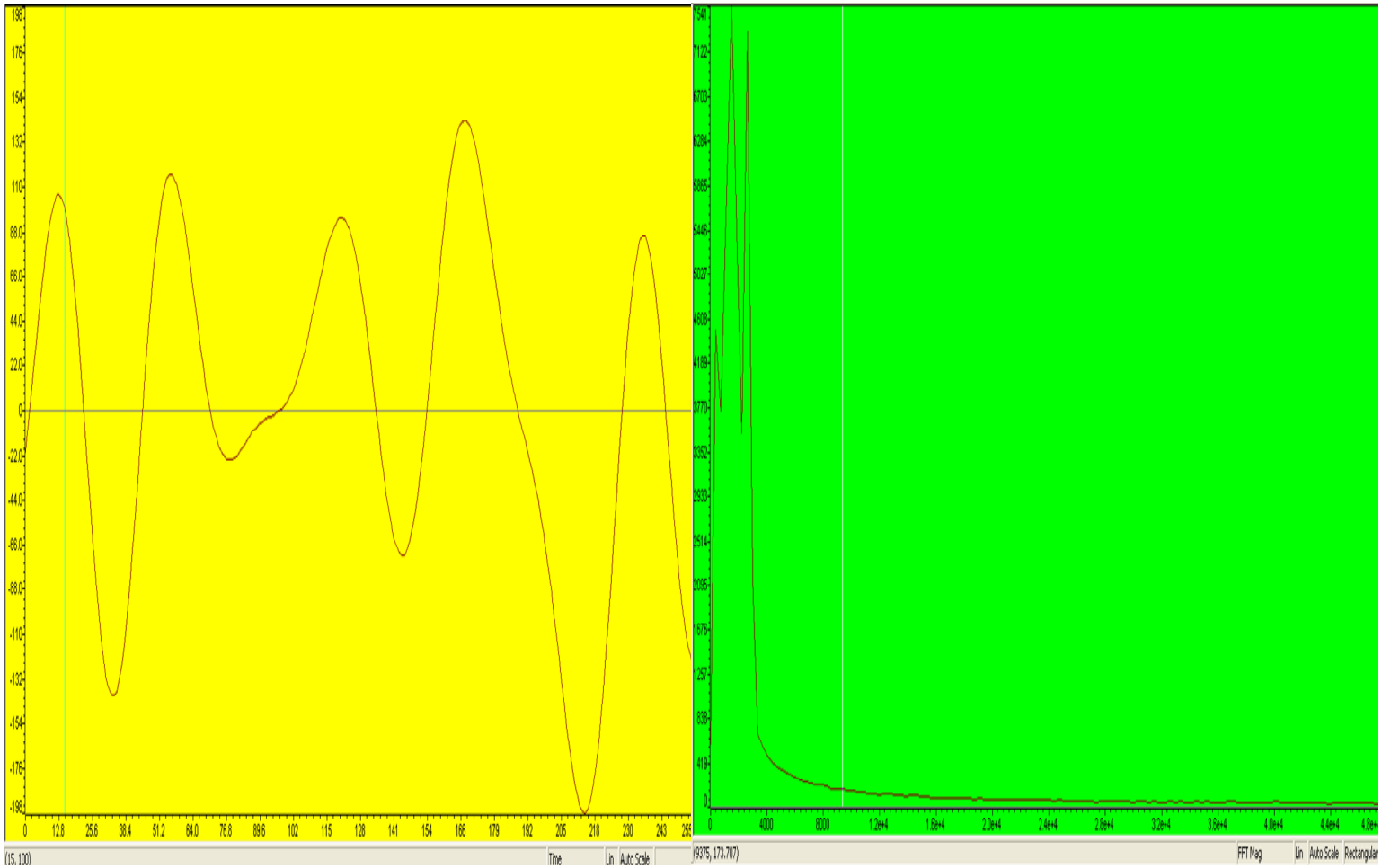

Figure 15. Time and frequency response of regenerated original signal on receiver.

show the results of implementation, respectively. This implementation was conducted successfully. Carrier frequency was detected by “random carrier frequency detection algorithm” at receiver side.

CONCLUSION

During the past 10 years, significant developments have been made in the DSP and converter technologies. These developments have made it possible for DSP's to be used for underwater communication applications.

In this paper, an underwater acoustic communication implementation was performed by using the DSP technology. A digital solution for underwater communication is proposed as well. The proposed digital solution provided a performance superior to the conventional analog technology and was developed via the transmitter and receiver sides on two TMS320VC5509A DSK boards by using upper sideband - suppressed carrier (SSB - SC) and random carrier frequencies. In addition to a more reliable underwater acoustic communication was implemented a continuously changing carrier frequency using random carrier frequency generation and detection algorithms. The results were obtained using SSB modulation with only two random carrier frequencies (8 kHz, 16 kHz) in a test pool due to hardware and transducer limitations. Being a prototype model, in contrast to common practice a relatively weaker transducer was used. Nevertheless, the current application has met the real-time signal processing requirements for underwater acoustic communication.

REFERENCES

Baggeroer A (1984). Acoustic telemetry – an overview, IEEE J. Oceanic. Eng. 9: 229-235.

Brekhovskikh L, Lysanov Y (1982). Fundamentals of Oceans Acoustics, New York – Springer.

Brüel and Kjær Inc. (1992). Technical Documentation – Hydrophones Types 8103, 8104, 8105, 8106.

Brüel and Kjær Inc. (2009). Calibration Chart for Hydrophones Types 8103 – D – 005.

Catipovic J (1990). Performance limitations in underwater acoustic telemetry, IEEE J. Oceanic Eng., 15: 205-216.

http://yb1zdx.arc.itb.ac.id/data/OWP/arrl-books/arrl-handbook-2005/16.pdf (2009). DSP and Software Radio Design.

Istepanian RSH, Stojanovic M (2002). Underwater Acoustic Digital Signal Processing and Communication Systems, Kluwer Academic Publishers.

Quazi A, Konrad W (1982). Underwater Acoustic Communications, IEEE Comm. Magazine, pp. 24-29.

Reson Inc. (2009). Catalogue Standard Transducers and Hydrophones, pp. 125 -129.

Spectrum Digital Inc (2005). TMS320VC5509A DSK Technical Reference.

Stajanovic M (1996). Recent advances in high rate underwater acoustic communications, IEEE J. Oceanic Eng., pp. 125-136.

Texas Instruments Inc (2002). TLV320AIC23 Stereo Audio Codec Data Manual.

Texas Instruments Inc (2006). TMS320C55x DSP Library Programmer’s Reference.

Yagnamurthy NK (2003). Jelinek HJ, A DSP Based Underwater Communication Solution, OCEANS, 1: 120-123, ABD.

Zielinski A (2004). Communications Underwater, Inv. P, J. Hydroacoustics, 7: 235-252, Gdynia